



HAL
open science

Fumarolic-like activity on carbonaceous chondrite parent body

Clément Ganino, Guy Libourel

► **To cite this version:**

Clément Ganino, Guy Libourel. Fumarolic-like activity on carbonaceous chondrite parent body. *Science Advances*, 2020, 6 (27), pp.eabb1166. 10.1126/sciadv.abb1166 . hal-02913703

HAL Id: hal-02913703

<https://hal.science/hal-02913703>

Submitted on 10 Aug 2020

HAL is a multi-disciplinary open access archive for the deposit and dissemination of scientific research documents, whether they are published or not. The documents may come from teaching and research institutions in France or abroad, or from public or private research centers.

L'archive ouverte pluridisciplinaire **HAL**, est destinée au dépôt et à la diffusion de documents scientifiques de niveau recherche, publiés ou non, émanant des établissements d'enseignement et de recherche français ou étrangers, des laboratoires publics ou privés.

PLANETARY SCIENCE

Fumarolic-like activity on carbonaceous chondrite parent body

Clément Ganino^{1*} and Guy Libourel^{2,3}

Comparative planetology studies are key for understanding the main processes driving planetary formation and evolution. None have been yet applied to pristine asteroids formed in the solar protoplanetary disk, mainly because of their comminution during their 4.5-billion-year collisional lifetime. From remarkable textural, mineralogical, chemical, and thermodynamic similarities, we show that the high-temperature Kudryavy volcano fumarolic environment from Kurile Islands is a likely proxy of the Fe-alkali-halogen metasomatism on the CV and CO carbonaceous chondrite parent bodies. Ca-Fe-rich and Na-Al-Cl-rich secondary silicates in CV and CO chondrites are, thus, inferred to be fumarolic-like incrustations that precipitate from hot and reduced hydrothermal vapors after interactions with the wallrocks during buoyancy-driven Darcy flow percolation. These vapors may originate from the progressive heating and devolatilization of a chondritic protolith on their parent body or are remnant of the cooling of residual local nebular gases at the time of their primary planetesimal accretion.

INTRODUCTION

Understanding the formation and the evolution of the planetesimals, the first building blocks of our planetary system, is a crucial problem in planetary science. During the first tens of millions of years following accretion, it is generally believed that temperatures on chondrite parent bodies increased as a result of the decay of short-lived radioisotopes such as ²⁶Al [e.g., (1)]. This warming resulted in the melting of ice and mobilization of fluids that aqueously altered pristine chondritic material (2, 3). Further temperature increases resulted in metamorphism of pristine material to various degrees (4, 5). Still, the exact nature of these secondary fluid-assisted thermal processes, as well as the nature of the involved fluid (vapor transport or pervasive liquid water alteration), is the subject of vigorous debate. Despite their obliterating role, these secondary processes are, however, particularly useful since they shed light on chondrite parent body internal structure and bring constraints on the accretion age of these primordial bodies.

In general, mineralogical and chemical survey of secondary phases in chondritic meteorites allows, using thermodynamic, geochemical, and radio chronological parameterizations, the evaluation of the formation conditions and the timing of these minerals. While providing valuable models of parent body alteration, these studies are often incomplete in terms of the sequence of the processes involved, and in no case allow a detailed view of the real timing of the fluid percolation. Comparative planetology studies show that a leap forward can be accomplished by the use of natural analogs. “Analogous” meaning similar and not identical, here we show that the high-temperature fumarolic environments of the Kudryavy volcano (Kurile Islands, Russia) can be used as a unique analog of the hydrothermal activity on CV (Vigarano-type) and CO (Ornans-type) chondrite parent bodies. Owing to this analogy, it is thus possible to infer the physicochemical conditions responsible for the formation

of the secondary phases in carbonaceous chondrites, to better constrain the phenomenology of their parent body alteration.

RESULTS

Fe-alkali-halogen secondary phases in CV and CO chondrites versus Kudryavy volcano fumarolic incrustations

Among the carbonaceous chondrite group assumed to be one of the most pristine, the CV and CO chondrites show documented evidence of alteration effects (6, 7). Numerous surveys [see recap in (7)] have shown matrix, refractory Ca-Al-rich inclusions (CAIs) and chondrules of CV and CO chondrites have all been affected by a so-called Fe-alkali-halogen metasomatism that has resulted in the formation of a wide range of secondary, dominantly anhydrous minerals. It has been shown that conditions of formation of these secondary phases in CV chondrites encompass the same range of temperature, oxygen fugacity, and silica activity (8, 9), suggesting that reduced (CV_R) and oxidized (CV_{Ox}) dichotomy would refer to modal abundance of their secondary phases (i.e., magnetite) rather than their metamorphic conditions of formation. The secondary minerals include abundant Ca-Fe-rich silicates: diopside-ferrosalite, hedenbergite, andradite, fayalite, kirschsteinite, wollastonite, rankinite, and larnite; oxides: magnetite, hercynite, and corundum; sulfides: troilite and pentlandite; Ca-phosphates; Fe-Ni-Co metal: awaruite and wairauite; carbides: cohenite; Na-Al-Cl-rich feldspathoids: nepheline, sodalite, and wadalite; and rare phyllosilicates: talc, tremolite, anthophyllite, and serpentines. Ca-Fe-rich pyroxenes (i.e., hedenbergite) are, by far, the most dominant secondary phases and are frequently found in association with andradite, wollastonite, and/or kirschsteinite (3, 8, 10). CO chondrites show also substantial evidence of alteration events, but the degree and extent of alteration are, in general, less than those for the CV chondrites (7, 11). The textural features of these secondary phases are the same in both groups and correspond to (Figs. 1 to 3) (i) altered chondrules or CAIs showing concentration of Ca-Fe silicates around these components and a more sparse distribution in the matrix away from them, (ii) micrometer-sized porous and polycrystalline nodules or patches scattered in the matrix, (iii) fine polycrystalline veinlets forming, in some cases, an imbricated network in the matrix or in dark inclusions, (iv) larger delineated

Copyright © 2020
The Authors, some
rights reserved;
exclusive licensee
American Association
for the Advancement
of Science. No claim to
original U.S. Government
Works. Distributed
under a Creative
Commons Attribution
NonCommercial
License 4.0 (CC BY-NC).

¹Université Côte d'Azur, OCA, CNRS, IRD, Géoazur, 250 rue Albert Einstein, Sophia-Antipolis, 06560 Valbonne, France. ²Université Côte d'Azur, OCA, CNRS, Lagrange, Boulevard de l'Observatoire, CS 34229, 06304 Nice Cedex 4, France. ³Hawai'i Institute of Geophysics and Planetology, School of Ocean, Earth Science and Technology, University of Hawai'i at Mānoa, Honolulu, HI 96821, USA.

*Corresponding author. Email: ganino@unice.fr

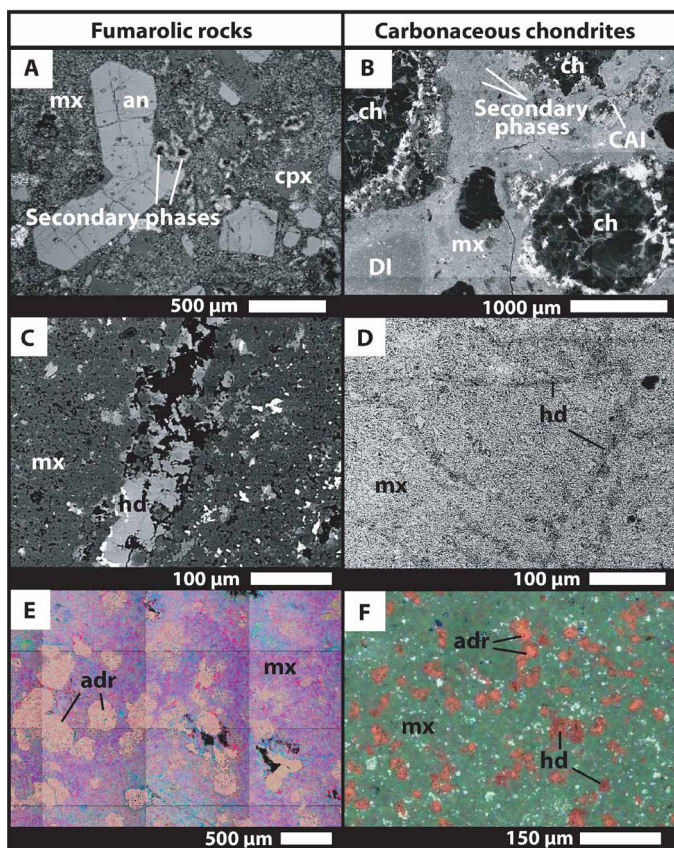


Fig. 1. Backscattered scanning electron microscopy (BS-SEM) observation of high-temperature fumarolic incrustations from Kudryavy volcano, and secondary minerals in CV chondrites. (A) Large view of primary basaltic andesite porphyritic texture of fumarolic incrustations from Kudryavy volcano with corroded clinopyroxene and plagioclase (anorthite) bathed in a fine-grained microlithic groundmass and showing the scattered Ca-Fe-rich secondary phases. (B) Large view of Bali CV chondritic texture from secondary minerals in CV chondrites with chondrules (ch), CAI, and dark inclusion (DI) cemented by a fine-grained matrix (mx) and hosting Ca-Fe-rich secondary phases. (C) Vein filled with hedenbergite-diopside assemblage within the plagioclase and pyroxene groundmass of fumarolic incrustations from Kudryavy volcano. (D) Detail of a vein network filled with hedenbergite within the fine-grained olivine (fa50) groundmass of a dark inclusion of Allende from secondary minerals in CV chondrites. (E) SEM backscattered electron images coupled with energy-dispersive x-ray chemical maps of hedenbergite and andradite (reddish) patches in the groundmass of Kudryavy fumarolic rock sample 11C (red, calcium; blue, silicon; green, iron; light blue, aluminum; pink, sulfur; yellow, sodium; orange, magnesium; light green, chlorine; violet, titanium; purple, potassium). (F) Backscattered electron (BSE)-SEM images from secondary minerals in CV chondrites, coupled with energy-dispersive x-ray chemical maps of hedenbergite and andradite (reddish) patches in the matrix of Allende (red, calcium; blue, aluminum; green, iron). adr, andradite; an, anorthite; cpx, "primary" magmatic clinopyroxene; hd, hedenbergite.

area (veins or dark inclusions) showing radial or lateral mineralogical zoning, (v) polycrystalline rims around preexisting Mg-rich chondrule olivine grains scattered in the matrix, and (vi) incrustations in larger cavities (pores) with nearly euhedral minerals forming negative crystals. When data are available, matrix abundance and bulk porosity of carbonaceous chondrites are highly variable [between 1% porosity in Efremovka and 25 to 30% for Allende and Mokoia; see (10)].

Synopsis of the occurrence and composition of these secondary phases may be found elsewhere [e.g., (6–8, 10–14)] and is not

reiterated here. Despite this extensive work, the environment and conditions of their formation remain however controversial. Palme and Wark (15) were among the first to favor a nebular origin for several secondary features (e.g., Fe-alkali-halogen metasomatism of CAIs and formation of fayalitic olivine rims around forsteritic grains). Observed intergrowths of nearly pure hedenbergite and diopside-hedenbergite and the presence of andradite have also been assigned to a high-temperature ($\approx 1000^\circ\text{C}$) nebular origin (16). Although these minerals assemblages are clearly restrictive in term of temperature, their proposed nebular formation has progressively fallen into disuse. From textural and mineralogical observations and chemical analyses, Bischoff (17) found evidence for these secondary phases to have originated from preaccretionary aqueous alteration processes that occurred in small precursor planetesimals before formation of the final parent bodies, an intermediate model between gas-solid interaction in the nebula and processes that occurred in the parent body. The debate was stirred up again on the basis of the thermodynamic modeling of mineral equilibria and the oxygen isotopic composition when it was suggested that secondary phases (i.e., Ca-Fe-rich pyroxenes, andradite, fayalite, phyllosilicates, and magnetite) resulted from low temperatures ($<300^\circ\text{C}$) aqueous fluid-rock interaction in an asteroidal setting (3, 13), in which reduced and oxidized CV chondrites witness different physico-chemical conditions. This low-temperature model has been challenged recently (8) by showing that Ca-Fe-rich phases in reduced and oxidized CV have formed at higher temperature (210° to 610°C , and possibly higher) and in similar reduced conditions near the iron-magnetite redox buffer under low $a\text{SiO}_2$ [$\log(a\text{SiO}_2) < -1$]. In this model, the various CV lithologies, which may be in part applied to CO chondrites, are inferred to be fragments of an asteroid percolated heterogeneously via porous flow of hot and reduced hydrothermal fluids. To sum up, although there is a general agreement that parent body alteration is a fundamental process in the evolution and the formation of secondary phases of CV and CO carbonaceous chondrites, there is, however, no consensus neither on the composition and the nature of the fluids involved nor if we should consider one or several generations of parent bodies (18).

Kudryavy volcano consists of a small cone located in the northern end of Iturup island in the Kurile volcanic arc. The last large eruption occurred in 1883 and produced basaltic andesite flows, but small-scale phreatic eruption occurred more recently in 1999 (19). The Kudryavy basaltic andesite flows are composed of rare olivine, orthopyroxene (hyperstene), clinopyroxene (augite), plagioclase (labradorite to bytownite), and titanomagnetite (20) with porphyritic textures with fine-grained microlithic groundmass (Figs. 1 and 2), its chemical composition being typical of the calc-alkaline serie. Kudryavy volcano probably has a several-decade period of sustained high-temperature fumarolic activity (up to 920° to 940°C measured in 1992) and degassing of magma, which have been, at least for the last 30 years, regularly sampled for gases and condensates (20–23).

Its gas chemistry is typical of high-temperature subduction zone volcanoes with relative uniform $\text{H}_2\text{O}/\text{CO}_2$ ratios between 40 ± 10 and 70 ± 15 , $\text{H}_2/\text{H}_2\text{O}$ in the range of 10^{-2} between the fayalite-magnetite-quartz (FMQ) and nickel-nickel oxide (NNO) mineral buffer curves, CO_2/S (or C/S) and S/Cl ratios of 1 ± 0.3 and 4 ± 1 , respectively, and HCl concentration amounting to 0.5 to 1 mole percent (mol %) (21, 22).

Despite the complexity of the fumarolic environments, it has been shown that three different types of the alteration of the Kudryavy fumarolic rocks prevail when (i) volcanic gas directly reacts with the

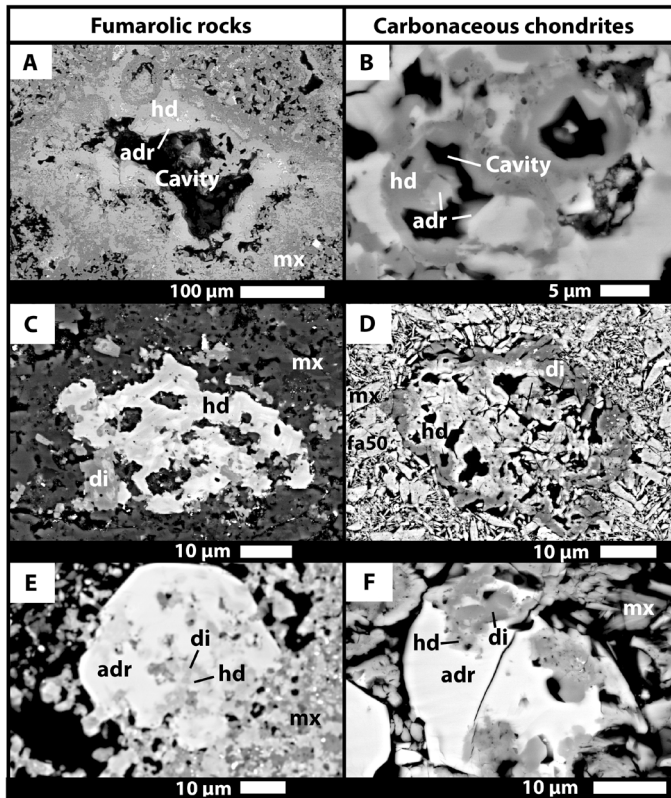


Fig. 2. BSE-SEM observation of high-temperature fumarolic incrustations from Kudryavy and secondary minerals in CV chondrites. (A) Crusted cavity in the Kudryavy andesite groundmass with concentric filling of hedenbergite and andradite. Euhedral andradite or hedenbergite protrude from cavity walls forming negative crystals. (B) Crusted cavity with concentric filling of hedenbergite and andradite in Allende CV chondrite. Notice the similarities with the fumarolic incrustations. (C) Patch of hedenbergite and diopside within the Kudryavy andesite groundmass. (D) Patch of hedenbergite and diopside within the matrix of Allende CV chondrite. (E) Euhedral andradite with hedenbergite and diopside inclusion at cavity walls forming negative crystals. (F) Euhedral andradite with hedenbergite and diopside inclusion within the matrix of Allende forming negative crystals. Similarities between (E) and (F) are striking. di, diopside; fa50, fayalite 50.

rock at high temperatures (900° to 500°C), forming a first generation of incrustations, (ii) oxidized volcanic gas, resulting from mixing with the atmosphere, directly reacts with the rocks at intermediate temperatures (500° to 300°C), and (iii) acidic leaching of the rocks by highly contaminated meteoric water remobilizes previously formed sublimates and/or incrustation deposits together with the precipitation of secondary incrustations (20, 21, 24).

Focusing only on the higher-temperature interactions where no atmosphere mixing exists (as attested by magmatic redox conditions close to the FMQ buffer and oxygen isotopic compositions typical of magmatic vapors associated with subduction-related arc volcanism), the mineralogy of incrustations in representative fumarolic rock samples (20, 21, 23) is strikingly similar to the aforementioned secondary phases of CV and CO chondrites. It includes andradite, diopside-ferrosalite, hedenbergite, Fe oxides, hercynite, wollastonite, cristobalite, and tridymite, here replacing the primary magmatic minerals. Diopside/salite-hedenbergite-andradite associations are found to overwhelmingly dominate the mineralogy of Kudryavy in-

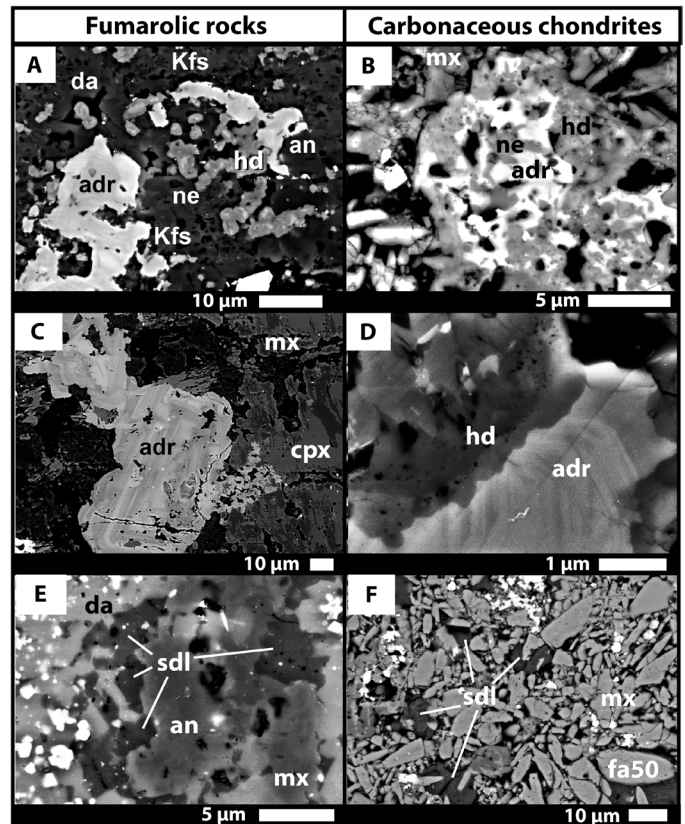


Fig. 3. BSE-SEM observation of high-temperature fumarolic incrustations from Kudryavy and secondary minerals in CV chondrites. (A) Assemblage of Ca-Fe-rich minerals (andradite and hedenbergite) with Na-Al-rich silicates (nepheline and davyne) in the andesite groundmass. (B) Assemblage of Ca-Fe-rich minerals (andradite and hedenbergite) with Na-Al-rich silicates (nepheline) in the matrix of Allende CV chondrite. (C) Andradite chemical zoning pattern (pure andradite in light gray and grossular-rich composition in darker gray) in Kudryavy andesite incrustations. (D) Similar andradite zoning pattern here in contact with hedenbergite, within the porous matrix of Allende CV chondrite (pure andradite in light gray and grossular-rich composition in darker gray). (E) Patches of sodalite associated with davyne in Kudryavy andesite. (F) Patches of sodalite in the matrix of Allende CV chondrite. da, davyne; Kfs, K-feldspar; ne, nepheline; sdl, sodalite.

crustations in the same manner as Ca-Fe-rich secondary phases do in CV and CO chondrites. Similarly, they are intimately associated with assemblages of Na-Al-Cl-rich phases, i.e., albite, nepheline, and sodalite, with the notable addition of davyne, another tectosilicate containing both calcium sulfate and sodium chloride. If silica polymorphs and numerous sulfides are present as secondary phases, the absence of fayalite, kirschsteinite, larnite, metal, and phyllosilicates in the Kudryavy incrustations are, however, noticeable. Last, veins, altered phenocrysts with dissolution pits, and occurrence of numerous cavities in the microlithic groundmass filled with euhedral or layers of secondary phases (Fig. 2) indicate proactive dissolution/precipitation process.

Analogy between CV chondrites parent body hydrothermal activity and Kudryavy high-temperature fumarolic environments

Incrustations from Kudryavy fumarolic rocks have noteworthy similarities with the secondary phases of CV and CO chondrites not

only in terms of their mineralogy and chemistry but also in terms of the intensive parameters controlling these several assemblages.

Mineral chemistry

Mineral chemistry of secondary phases is unexpectedly similar in these two different settings (Fig. 4). Ca-Fe pyroxene, wollastonite, and feldspathoid, analyzed in CV and CO chondrites (3, 13, 25–27), all show the same ranges of chemical variations as those observed in the Kudryavy fumarolic rocks. Ca-rich pyroxenes varying from diopside to hedenbergite compositions in Kudryavy incrustations encompass the same range of compositions as the one observed in CV and CO carbonaceous chondrites. Mineralogical zoning in these pyroxenes is also similar, with a hedenbergite core surrounded at crystal edge by complex and irregular oscillatory zoning of iron-depleted pyroxene. Concentrations of Na_2O and Al_2O_3 in these secondary pyroxenes are also relatively high in both settings. Ca-Fe garnets in both type of environments show also same range of variations from almost pure andradite to grossular-rich compositions (20, 28) with sometimes occurrences of oscillatory zoning depending on their growth location (Fig. 3). In both settings, wollastonite and andradite are intimately associated. Last, Na-Al-silica-poor phase compositions: nepheline and sodalite (Fig. 3), are

also matching in the two sites, with similar enrichments in iron (as NaFeSiO_4 end member) in both phases and potassium depletions ($\text{Na}/\text{K}_{\text{atomic}}$ ratio > 3) in nepheline (table S1).

Texture

Both settings are characterized by heterogeneous textures of alteration with evidence for metasomatism (secondary phases) generally restricted to distances of a few hundred micrometers. Ca-Fe-silicates, Fe oxides, sulfides, Na-Al-Cl-rich feldspathoid phases in both carbonaceous chondrites (6–8, 13, 27, 29), and Kudryavy fumarolic rocks (20, 23, 30) are intimately associated under similar types of texture (Figs. 1 and 2): (i) overgrowth or pseudomorph on preexisting minerals, replacement of glassy or crystallized preexisting phases in matrix, chondrule mesostases, and refractory inclusions or in microlithic groundmass and phenocrysts; (ii) micrometer-sized porous polycrystalline patches dispersed in the fine-grained matrix; (iii) fine veinlets forming imbricated network in the matrix or inclusions; and (iv) larger delineated area (veins or dark inclusions) showing radial or lateral mineralogical zoning. These textural similarities are even more convincing if euhedral zoned crystals of andradite (or hedenbergite) growing in cavities of the volcanic rock or meteorites are considered. Euhedral andradites or hedenbergites

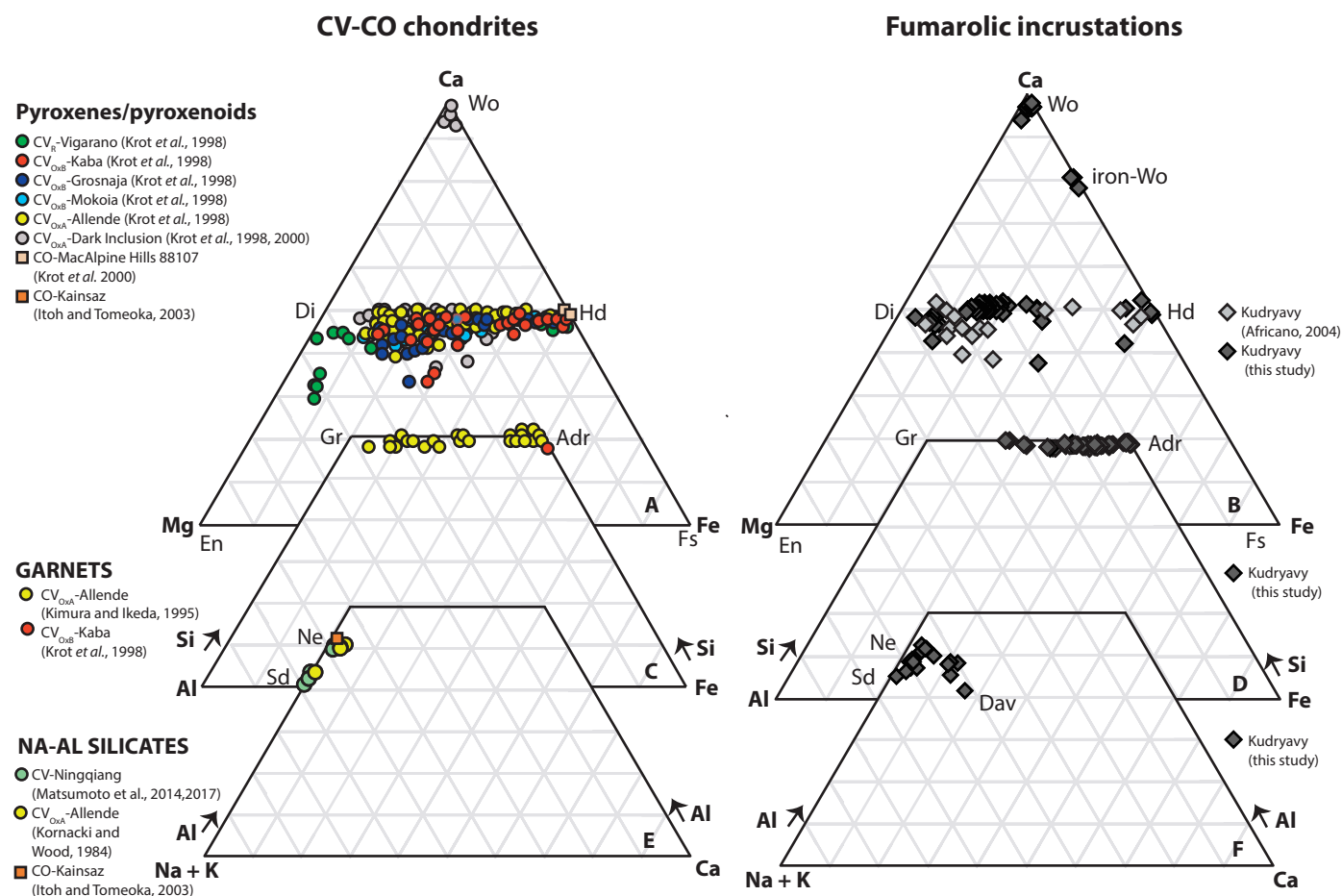


Fig. 4. Mineral composition. Pyroxene and pyroxenoid (A and B), garnet (C and D), and Na-Al-rich silicates (E and F) from CV-CO chondrites (A, C, and E) and from fumarolic incrustations of the Kudryavy volcano, Kurile Islands (B, D, and F). Similar phases with comparable range of composition are present in both environments. Wollastonite (wo), diopside, hedenbergite, andradite, grossular (gr), nepheline (ne), and sodalite (sd). Fe-rich wollastonite (B) and davyne (F) are only documented in Kudryavy and not in CV-CO chondrites.

often protrude from cavity walls or form negative crystals in micrometer-sized porous polycrystalline patches dispersed in the “unaltered” fine-grained matrix (Figs. 1 and 2) (31).

Intensive parameters

Beyond these similarities, the most convincing features supporting this analogy rely very likely on the fact that the same set of intensive parameters (i.e., $a\text{SiO}_2$ - $f\text{O}_2$ - T) controls these several assemblages in both these terrestrial and extraterrestrial environments. Among these, the andradite-hedenbergite assemblage \pm wollastonite \pm magnetite \pm sulfides is of particular interest. From experimental and thermodynamic analyses in the system Ca-Fe-Si-O, Gustafson (32) has shown that andradite and hedenbergite are stable over a range of $\log f\text{O}_2$ and T at low total pressure. Ganino and Libourel (8) recently complemented this view by establishing that the silica activity of the system is another key parameter controlling the stability field of andradite relative to hedenbergite. If andradite is stable at high temperature in oxidizing conditions at or close to silica saturation, it noticeably expands its stability field toward reducing conditions at low temperature in low-silica-activity environments, andradite being costable with iron and magnetite (8). That is the case for CV and CO chondrites, in which andradite and hedenbergite assemblages are often associated with magnetite \pm Fe-Ni alloy [e.g., awaruite; (3)] and sulfide in the presence of reduced carbon-rich material. From the thermodynamic parametrization of these associations (8), Ca-Fe-rich assemblages in CV and CO chondrites are inferred to have formed in reduced conditions near the iron-magnetite redox buffer at low $a\text{SiO}_2$ [$\log(a\text{SiO}_2) \ll -1$] and moderate temperature (210° to 610°C). In

addition to the cocrystallization of Na-Al-Cl-rich feldspathoids (nepheline and sodalite), which are good tracers of silica undersaturated environments in the parent body of CV and CO chondrites, very low silica activity conditions [i.e., $\log(a\text{SiO}_2) < -2$; see (33)] are also attested by the occurrence of rankinite, larnite, and wollastonite in the case of CV chondrites (8).

Using the same thermodynamic framework (Fig. 5), andradite-hedenbergite assemblages of Kudryavy fumarolic rock are reproduced at high temperature ($T > 650^\circ\text{C}$) and at intermediate silica undersaturation $-1 < \log(a\text{SiO}_2) \leq 0$ and redox conditions close to the FMQ buffer, i.e., $-17 < \log f\text{O}_2 < -12$. These inferred conditions are consistent with fumarole gas measurements and estimates (21, 22), indicative of elevated temperature of crystallization circa 900°C in more oxidizing conditions close to the FMQ buffer curve with $\log(f\text{H}_2/f\text{H}_2\text{O})$ values in the range of -2.0 to -2.5 that lie between the FMQ buffer and the NNO buffer (21). The mild silica undersaturation reigning in the Kudryavy fumarolic system by comparison with the CV/CO environments is also consistent with a unique T - $a\text{SiO}_2$ trend (Fig. 5) close to the nepheline/albite silica activity buffer curve, as indicated by the occurrence of the nepheline-albite-sodalite-davyne assemblages.

DISCUSSION

Evidences for fumarolic-like activities on carbonaceous parent bodies

The rarity in terrestrial environments of Ca-Fe-rich secondary phases in close association with Na-Al-Cl-rich minerals, and their noticeable

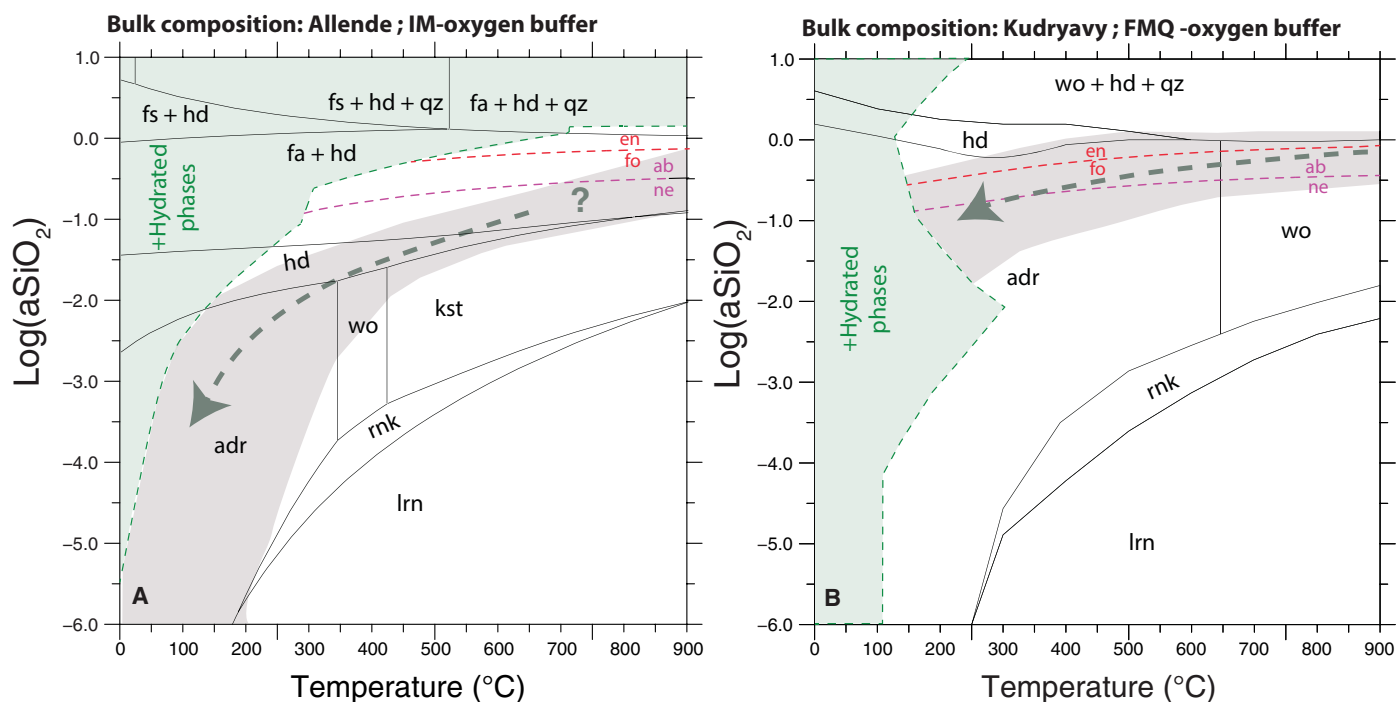


Fig. 5. Silica activity versus temperature diagrams of secondary mineral stability fields from both CV chondrite and Kudryavy fumarolic incrustation settings. (A) Mineral stability in the systems Ca-Fe-Si-O without water (black) and Ca-Fe-Si-O-H with excess water (green). Stability fields are calculated at IM buffered redox conditions and an indicative pressure of 2000 bar. The silica activity buffer curve nepheline/albite is also plotted. Characteristic Ca-Fe-rich assemblages in CV3 chondrites depict $\log(a\text{SiO}_2)$ - T pathway for each CV3 lithologies and fixed redox conditions [see also (8)]. Green lines and green area mark the stability fields of hydrous phases. (B) Similar plot with Kudryavy setting assuming FMQ buffered redox conditions. In both plots, a single trend matches the diversity of Ca-Fe secondary phases (gray area and dashed arrow), suggesting these secondary phases in both terrestrial and extraterrestrial environments obey to the same set of intensive parameters [$\log f\text{H}_2/f\text{H}_2\text{O}$, $\log f\text{O}_2$, $\log(a\text{SiO}_2)$, T]; see text for explanations.

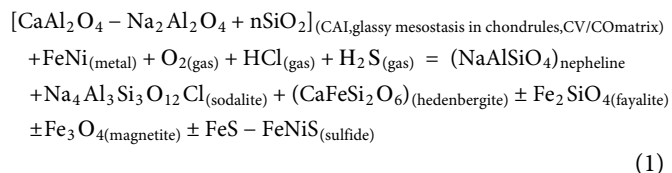
similarities with CV and CO secondary phases cannot be fortuitous and allows us to bring a fresh look on the Fe-alkali-halogen metasomatism operating on CV and CO chondrite parent bodies. Our survey, consistent with those of the literature, revealed that nepheline/sodalite and various Ca-Fe-rich secondary minerals are intimately intergrown with each other (Fig. 3). This suggests that all these minerals formed simultaneously in chondrite parent bodies during the same alteration process (28, 29). Detailed chemistry confirmed this contemporaneity with enrichments of iron in Na-Al-Cl-rich secondary phases (i.e., Fe in nepheline, very likely as Fe³⁺), and of Na and Al in the Ca-Fe-rich ones (i.e., Na and Al in diopside-hedenbergite, or Al in andradite; table S1). Similarly, oxygen isotopic compositions of both Ca-Fe-rich and Na-Al-Cl-rich secondary minerals from either matrix, chondrules, or CAIs of Allende (CV3) chondrites plot along on a same mass-dependent fractionation line with a slope of ~0.5 and Δ¹⁷O of -2.6 ± 2.6‰ (average ±2 SD), consistent with the formation of these phases in a same alteration setting (34). The same is observed for MAC 88107 CO3-like chondrite for which the oxygen isotopic compositions of secondary phases plot on a unique mass-dependent fractionation line with a slope of ~0.5 and Δ¹⁷O of -1.6 ± 0.9‰.

Assuming an asteroidal environment, the question arises now about the nature of the fluid responsible for such Fe-alkali-halogen metasomatism: vapor transport [e.g., Fuchs (31)] or pervasive liquid water alteration [e.g., Krot *et al.* (3)], which comes down to a temperature and fluid density issue. Typical density ranges at magmatic-hydrothermal conditions on Earth are ~0.001 to 0.35 g/cm³ and 0.35 to 1.0 g/cm³ for vapor and liquid phases, respectively, and this parameter controls mineral solubility (35). Carbonaceous chondrites have compositions that are within 10% of the solar photosphere for most elements, including the most soluble elements (36, 37), suggesting that fractionation of the soluble elements has not occurred and that extensive alteration within asteroids has not modified bulk carbonaceous chondrite chemistry. This isochemical alteration is difficult to reconcile with large-scale flow of liquid water (open system alteration) even if low temperatures are considered to avoid the fractionation of the most soluble elements (11, 38). Instead, for Bland *et al.* (37), unfractionated soluble elements hint for very limited fluid flow, indicating a closed system at scales larger than 100 μm, consistent with data from oxygen isotopes and chondrite petrography. Very limited and short-distance liquid water flow is predicted even over millions of years in a high-porosity, water-saturated asteroid having a high thermal gradient, if the extreme fine grain size of primitive chondritic materials and their correlative low permeability (in the range of 0.1 to 10 μD) are taken into account (37). However, this closed-system alteration cannot be reconciled with the spread of the secondary minerals along a single-oxygen mass-dependent fractionation line as it is observed in CV and CO chondrites, if interactions occurred very locally between the liquid water and chondrules, CAI, or matrix, which all have variable oxygen isotope ratios (e.g., Δ¹⁷O).

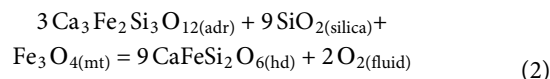
Here, we challenge these classical views of low-temperature liquid water alteration in carbonaceous parent bodies. By analogy with the Kudryavy volcano rocks, we infer that Ca-Fe-rich and Na-Al-Cl-rich secondary phases in CV and CO chondrites are fumarolic-like incrustations that precipitate from hot vapors after interactions with the wallrock during buoyancy-driven Darcy flow percolation (8). The present reasoning lies on the equilibrium concept commonly argued to apply for volcanic reactive gases expanding and interacting with rock material because reactions between component species are fast

and efficient (39). It should be kept in mind, however, that if it is certainly reasonable and appropriate to promote in the following a case for gas reactions as opposed to liquid water-phase reactions, the real understanding of high-temperature gas-solid reactions would require an in-depth analysis of the speciation of the major and minor components of the multicomponent gas mixture together with a description of the involved chemisorption reactions (24), a task clearly beyond the scope of this study and which will necessitate a dedicated study.

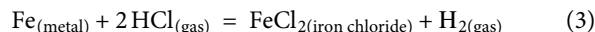
Restricting ourselves to a pure petrological perspective, the vapor buffering and the hedenbergite/andradite crystallization in CV chondrites have redox conditions estimated close to the iron-magnetite-reduced environment and a chemistry characterized by CO/CO₂ ≈ 1, H₂/H₂S ≈ 5 × 10³, and H₂/H₂O ≈ 5 with some mole fractions of HCl (8). This complex permeability-driven interaction between gas and CV/CO wallrock phases can be approximated by a type of reaction like



and the subsequent formation of andradite from hedenbergite (8) according to the following reaction



In this scenario, the mobility of iron is provided by the reactive HCl_(vapor) with the FeNi metal of the carbonaceous chondrites according to



and the rapid volatilization of FeCl₂ above ≈500°/600°C under reducing conditions (40), while iron sulfides are stable in the same conditions. Similarly, the inferred high vapor pressures, e.g., PHCl_{gas} and PH₂S_{gas} and the high-temperature conditions should favor the relative mobility (leaching) of some other major elements—Na, Ca, Al (very likely as chlorine gas species), and Si (as oxide gas species)—from chondrule mesostasis and, in a less extent, from CAI minerals (3, 8, 10, 12).

Several other textural and modal features of CV/CO chondrites can also be explained in the light of this model such as (i) the occurrence of euhedral and negative crystals in cavities formed in a similar way as fumarolic sublimates, (ii) the small-scale isochemical alteration irrespective of the nature of the substrate (matrix, CAI, or chondrules), (iii) the variable distribution of the secondary phases either in isolated patches and veinlets in the matrix or in peripheral cracks around chondrules/CAIs according to the local chondrite permeability, and (iv) the positive correlation between the modal abundances of secondary Ca-Fe-rich phases and Fe-Ni metal in CV chondrites (41). It remains to understand how hydrated secondary phases and phyllosilicates are positioned within the framework of this model. It is generally assumed that hydrated secondary phases

in CV chondrites were dehydrated and recrystallized by subsequent (prograde metamorphism) high temperatures (42, 43).

In any case, a comparison of our results with those inferred for other metamorphic/thermal sensors [oxide/sulfide mineralogy and iron valence study (44), structure of the polyaromatic carbonaceous matter determined by Raman spectroscopy (9, 45)] would be very valuable.

If this scenario is correct, the effect of such a fumarolic-like activity should have also an effect on the bulk porosity of CV and CO chondrites. As pores in the matrix are clearly filled with euhedral of secondary Ca-Fe-rich crystals (Figs. 1 and 2) and that cracks around chondrules/CAIs are filled by the same secondary minerals [Fig. 1, and see also Fig. 1d in Doyle *et al.* (11)], we believe that this process also sealed the porosity by incrustation while being consistent with the antagonism between the occurrence of a porosity in a very low permeability medium as inferred for CV and CO chondrites (37). Facing a complex process (including dissolution, condensation, and/or mineral reactions), more experimental work is needed to quantify the effect of sealing and to decipher the pristine postaccretionary porosity.

Time scale for formation of secondary phases in CV and CO chondrites and model accretion ages of their parent bodies

Ca-Fe-rich secondary phases, e.g., kirschsteinite and fayalite, from CV (Vigarano, Efremovka, Asuka 881317) and CO (MacAlpine Hills 88107) chondrites yield well-resolved ^{53}Cr excesses from the in situ decay of extinct ^{53}Mn , with $(^{53}\text{Mn}/^{55}\text{Mn})_0$ initial ratios ranging from $(3.71 \pm 0.50) \times 10^{-6}$ to $(3.07 \pm 0.44) \times 10^{-6}$. These ratios correspond to Ca-Fe-rich secondary phase formation in CV chondrites between 3.2 and 4.2 million years (Ma) after CV CAIs (46) and to slightly younger formation ages for those of CO chondrites (11). Taken at face value, these ages are our present-day best estimates of the timing of CV and CO metasomatic alteration by hot reduced vapors.

By definition, parent body metasomatism must have occurred after accretion of that parent body. For CV and CO chondrite parent body, the start of accretion is constrained by the first peak in chondrule formation at ca. 2.0 to 2.3 Ma after CAIs (47, 48), and the final accretion cannot predate the formation of the youngest chondrules. Irrespective of the use of long- or short-lived radionuclide chronology for chondrule ages (47–50), this constrains the final stage of CV and CO chondrite parent body accretion to $> 2.92_{-0.43}^{+0.75}$ Ma after formation of CAIs. This modeled accretion age of the CV chondrite parent body is in agreement with the ^{26}Al - ^{26}Mg formation age of > 2.6 Ma for secondary grossular in the CAIs from the CV3 Allende chondrite (51). These modeled accretion ages are generally comparable to or slightly younger than the majority of ^{26}Al - ^{26}Mg ages of chondrules in each chondrite group. If correct, this suggests a rapid accretion of parent asteroid after the latest chondrule forming event (11, 49).

Even though the duration of accretion of chondrite parent bodies is poorly understood, the $(^{26}\text{Al}/^{27}\text{Al})_0$ ratios in the youngest chondrules from an individual chondrite group provide upper limits on ^{26}Al abundances available for heating up the corresponding parent asteroid by ^{26}Al decay. This ratio amounts to circa $(^{26}\text{Al}/^{27}\text{Al})_0 \approx 2\text{--}3 \times 10^{-6}$ or lower for CV and CO parent asteroids (49, 50) if one assumes that ^{26}Al was the only heat source of a chondrite parent body and was uniformly distributed in the protoplanetary disk with the canonical $^{26}\text{Al}/^{27}\text{Al}$ ratio of 5.25×10^{-5} . In these circumstances of relatively low ^{26}Al abundances available, none of the modeled thermal evolution of the CV- and CO-like

parent bodies with different radii heated only by decay of the short-lived radionuclide ^{26}Al is able to produce peak temperature in the innermost portion of these bodies in excess to $\approx 400^\circ\text{C}$ (11). These temperatures are too low to match those needed to crystallize these Ca-Fe-rich secondary phases, including hedenbergite- or kirschsteinite-bearing assemblages (8, 16). In addition, owing to the balance between the heat generated by decay of ^{26}Al and heat lost through radiation, the maximum temperature reached in large bodies > 50 to 100 km is largely controlled by their accretion time (and not their size) (11).

In the scope of the present analogy with the fumarolic environment from Kurile Islands and assuming relatively late accretion ages of CV and CO chondrite parent bodies, the present finding may also accredit a potential paradigm shift. Fluid-assisted metamorphism on the CV and CO parent bodies might not be considered as a continuous protracted event powered by ^{26}Al decay, but rather as resulting from hot hydrothermal activity pulses maybe as short as a few tens of years or so. This time scale, of the same order of magnitude as short hydrothermal activity inferred from ordinary chondrite parent body (52), is many orders of magnitude shorter than the million-year time scales implied by short-lived radioisotope chronometers.

It remains now to understand the origin of these hot reduced vapors. They can be originated from the progressive heating and devolatilization of a chondritic protolith, assuming that CV and CO chondrites represent the unprocessed crusts of internally differentiated early planetesimals that must have accreted within 1.5 Ma after CAIs (53). CV3 chondrites having a unidirectional magnetization have been interpreted as the unmelted crusts of internally differentiated early planetesimals heated primarily by the short-lived radioisotope ^{26}Al (54, 55). In this case, the metasomatic fluid can percolate rapidly through CV and CO chondrites from the deep interior of their parent asteroids, since Darcy flow calculations indicate that supercritical fluids at 900°C would move upward through the planetesimal at speeds in excess of 1 km year^{-1} (56). Otherwise, these hot reduced vapors could simply be remnants of residual local hot nebular gases at the time of the primary accretion CV and CO chondrite parent bodies, which then may percolate and interact upon cooling with the multicomponent dust aggregates (e.g., chondrules, CAIs, and fine-grained phases) during the lithification stage of CV and CO chondrites, in a similar way as nuées ardentes or pyroclastic flows consolidate into ignimbrites. Better age constraints of the youngest chondrules and Ca-Fe-rich secondary phases in carbonaceous chondrites will be, however, required to decide between these two paradigms.

MATERIAL AND METHODS

Samples

For this study, we focused on polished thin sections of carbonaceous chondrite-Vigarano type of Allende, Bali, and Kaba provided by the Museum National d'Histoire Naturelle (MNHN; Paris), and a thin section from Vigarano provided by the Smithsonian National Museum of Natural History (Washington, DC). We also inspected 10 samples of fumarolic incrustations from the Kudryavy volcano (Kuriles islands) provided by A. Bernard that were collected in August 1995 at depths of 10 to 30 cm near active fumaroles at temperatures up to $\sim 900^\circ\text{C}$. These samples are described in a dedicated paper (30).

Mineral characterization

Textural and mineralogical characterizations of the terrestrial and extraterrestrial samples have been undertaken at Observatoire de la Côte d'Azur using a scanning electron microscope (SEM) COXEM EM-30AX for prescreening. Detailed chemical analyses were performed at CEMEF MINES ParisTech-Nice (France) using a SEM FEI XL30 ESEM LaB6 operated at 20 kV and 200-nA beam current, equipped with a Bruker QUANTAX 655 detector with XFlash 6|30 technology silicon drift of 10 mm² at 129 eV (100 kilo counts per second). Bruker Microanalyser QUANTAX was associated with the software ESPRIT (semiquantitative analyses without standard by peak-to-background using ZAF matrix correction method). Additional chemical analyses of the secondary phases have been acquired using Field Emission Electron Probe Microanalyzer (EPMA) UH JEOL JXA-8500F operating at 20-kV accelerating voltage, 50-nA beam current, and 1-μm-sized beam at HIGP, University of Hawai'i at Manoa, Honolulu (USA). Fluorescence was calibrated to the K-lines of Mg in SC olivine (using a TAP crystal), Si in Rockport fayalite (TAP), Cr on magnesiochromite (LiFH), Fe in fayalite (LiF), and Mn in Verma garnet (LiF). Standardization was made for Fe and Si on Rockport fayalite (Fe_{1.9}Mn_{0.1}SiO₄; USNM85276), Mg on SC olivine (Mg_{1.8}-Fe_{0.2}SiO₄; NMNH111312), Mn on Verma garnet (Fe_{1.2}Mn_{1.7}Al₂Si₃O₁₂), and Cr on magnesiochromite (Mg_{0.7}Fe_{0.4}Cr_{1.6}Al_{0.4}O₄; NMNH117075), with counting times on peak (and each background) as follows: 90 s (45 s) for Mg, Cr, and Si; 30 s (15 s) for Mn; and 20 s (10 s) for Fe. The background fitted to the trace elements magnesium and chromium was an exponential function defined by Probe for EPMA v.929. ZAF matrix corrections (57) were applied. The detection limits were 0.02 weight % (wt %) for FeO and 0.01 wt % for all other oxides.

Thermodynamic analyses

The thermodynamic framework present here was obtained using the Domino program from the Theriak-Domino software (58), and the internally consistent thermodynamic datasets from Holland and Powell (59) were extended with kirschsteinite properties [see details in (8)]. This modeling lies on the equilibrium concept commonly been argued to apply for volcanic reactive gases expanding and interacting with rock material (39) because reactions between component species are fast and efficient. Thermochemical equilibrium modeling provides a reasonable basis to explain gas-solid reactions and their products in the fumarolic system (24). The results presented here (Fig. 5) used the bulk composition from Allende chondrite (60) and from Kudryavy volcano basaltic andesite (21) simplified to their Ca-Fe-Si-O components as inputs.

SUPPLEMENTARY MATERIALS

Supplementary material for this article is available at <http://advances.sciencemag.org/cgi/content/full/6/27/eabb1166/DC1>

REFERENCES AND NOTES

- G. J. MacPherson, A. M. Davis, E. K. Zinner, The distribution of aluminum-26 in the early solar system—A reappraisal. *Meteoritics*. **30**, 365–386 (1995).
- E. D. Young, R. D. Ash, P. England, D. Rumble III, Fluid flow in chondritic parent bodies: Deciphering the compositions of planetesimals. *Science* **286**, 1331–1335 (1999).
- A. N. Krot, M. I. Petaev, E. R. D. Scott, B.-G. Choi, M. E. Zolensky, K. Keil, Progressive alteration in CV3 chondrites: More evidence for asteroidal alteration. *Meteorit. Planet. Sci.* **33**, 1065–1085 (1998).
- W. R. Van Schmus, J. A. Wood, A chemical-petrologic classification for the chondritic meteorites. *Geochim. Cosmochim. Acta* **31**, 747–765 (1967).
- A. Brearley, R. H. Jones, Chondritic meteorites, in *Planetary Materials*, J. J. Papike, Ed. (Washington, DC Mineralogical Society of America, 1998), vol. 3.
- K. Tomeoka, D. Itoh, Sodium-metasomatism in chondrules in CO3 chondrites: Relationship to parent body thermal metamorphism. *Meteorit. Planet. Sci.* **39**, 1359–1373 (2004).
- A. J. Brearley, A. N. Krot, Metasomatism in the early solar system: The record from chondritic meteorites, in *Metasomatism and the Chemical Transformation of Rock, Lecture Notes in Earth System Sciences*, D. Harlov, H. Austrheim, Eds. (Berlin and Heidelberg, Germany, Springer-Verlag, 2013), pp. 659–789.
- C. Ganino, G. Libourel, Reduced and unstratified crust in CV chondrite parent body. *Nat. Commun.* **8**, 261 (2017).
- L. Bonal, E. Quirico, L. Flandinet, G. Montagnac, Thermal history of type 3 chondrites from the Antarctic meteorite collection determined by Raman spectroscopy of their polyaromatic carbonaceous matter. *Geochim. Cosmochim. Acta* **189**, 312–337 (2016).
- G. J. MacPherson, A. N. Krot, The formation of Ca-, Fe-rich silicates in reduced and oxidized CV chondrites: The roles of impact-modified porosity and permeability, and heterogeneous distribution of water ices. *Meteorit. Planet. Sci.* **49**, 1250–1270 (2014).
- P. M. Doyle, K. Jogo, K. Nagashima, A. N. Krot, S. Wakita, F. J. Ciesla, I. D. Hutcheon, Early aqueous activity on the ordinary and carbonaceous chondrite parent bodies recorded by fayalite. *Nat. Commun.* **6**, 7444 (2015).
- A. N. Krot, E. R. D. Scott, M. E. Zolensky, Mineralogical and chemical modification of components in CV3 chondrites: Nebular or asteroidal processing? *Meteoritics*. **30**, 748–775 (1995).
- M. Matsumoto, K. Tomeoka, Y. Seto, A. Miyake, M. Sugita, Nepheline and sodalite in the matrix of the Ningqiang carbonaceous chondrite: Implications for formation through parent-body processes. *Geochim. Cosmochim. Acta* **126**, 441–454 (2014).
- A. J. Brearley, Disordered biopyriboles, amphibole, and talc in the Allende meteorite: Products of nebular or parent body aqueous alteration? *Science* **276**, 1103–1105 (1997).
- H. Palme, D. A. Wark, CV-chondrites: High temperature gas-solid equilibrium vs. parent body metamorphism, in *Lunar and Planetary Science Conference* (1988), vol. 19, pp. 897–898.
- F. E. Brenker, A. N. Krot, Late-stage, high-temperature processing in the Allende meteorite: Record from Ca, Fe-rich silicate rims around dark inclusions. *Am. Mineral.* **89**, 1280–1289 (2004).
- A. Bischoff, Aqueous alteration of carbonaceous chondrites: Evidence for preaccretionary alteration—A review. *Meteorit. Planet. Sci.* **33**, 1113–1122 (1998).
- K. Jogo, M. Ito, S. Wakita, S. Kobayashi, J. I. Lee, Origin of the metamorphosed clasts in the CV 3 carbonaceous chondrite breccias of Graves Nunatak 06101, Vigarano, Roberts Massif 04143, and Yamato-86009. *Meteorit. Planet. Sci.* **54**, 1133–1152 (2019).
- M. A. Korzhinsky, R. E. Botcharnikov, S. I. Tkachenko, G. S. Steinberg, Decade-long study of degassing at Kudryavy volcano, Iturup, Kurile Islands (1990–1999): Gas temperature and composition variations, and occurrence of 1999 phreatic eruption. *Earth, Planets Sp.* **54**, 337–347 (2002).
- F. Africano, thesis, Université Libre de Bruxelles (2004).
- Y. A. Taran, J. W. Hedenquist, M. A. Korzhinsky, S. I. Tkachenko, K. I. Shmlovich, Geochemistry of magmatic gases from Kudryavy volcano, Iturup, Kuril Islands. *Geochim. Cosmochim. Acta* **59**, 1749–1761 (1995).
- T. P. Fischer, W. F. Giggenbach, Y. Sano, S. N. Williams, Fluxes and sources of volatiles discharged from kudryavy, a subduction zone volcano, Kurile Islands. *Earth Planet. Sci. Lett.* **160**, 81–86 (1998).
- F. Africano, A. Bernard, M. Korzhinsky, High temperature volcanic gas geochemistry (major and minor elements) at Kudryavy volcano, Iturup Island, Kuril arc, Russia. *Vulcânica*. **1**, 87–94 (2003).
- R. W. Henley, T. M. Seward, Gas–solid reactions in arc volcanoes: Ancient and modern. *Rev. Mineral. Geochemistry*. **84**, 309–349 (2018).
- A. S. Kornacki, J. A. Wood, The mineral chemistry and origin of inclusion matrix and meteorite matrix in the Allende CV3 chondrite. *Geochim. Cosmochim. Acta* **48**, 1663–1676 (1984).
- D. Itoh, K. Tomeoka, Dark inclusions in CO3 chondrites: New indicators of parent-body processes. *Geochim. Cosmochim. Acta* **67**, 153–169 (2003).
- M. Matsumoto, K. Tomeoka, Y. Seto, Nepheline and sodalite in chondrules of the Ningqiang carbonaceous chondrite: Implications for a genetic relationship with those in the matrix. *Geochim. Cosmochim. Acta* **208**, 220–233 (2017).
- M. Kimura, Y. Ikeda, Anhydrous alteration of Allende chondrules in the solar nebula II: Alkali-Ca exchange reactions and formation of nepheline, sodalite and Ca-rich phases in chondrules. *Proc. NIPR Symp. Antarct. Meteor.* **8**, 123–138 (1995).
- Y. Ikeda, M. Kimura, Anhydrous alteration of Allende chondrules in the solar nebula I: Description and alteration of chondrules with known oxygenisotopic compositions. *Proc. NIPR Symp. Antarct. Meteor.* **8**, 97–122 (1995).

30. C. Ganino, G. Libourel, A. Bernard, Fumarolic incrustations at Kudryavy volcano (Kamchatka) as a guideline for high-temperature (>850 °C) extinct hydrothermal systems. *J. Volcanol. Geotherm. Res.* **376**, 75–85 (2019).
31. L. H. Fuchs, Occurrence of wollastonite, rhönite, and andradite in the Allende meteorite. *Am. Mineral.* **56**, 2053–2068 (1971).
32. W. I. Gustafson, The stability of andradite, hedenbergite, and related minerals in the system Ca–Fe–Si–O–H. *J. Petrol.* **15**, 455–496 (1974).
33. I. S. E. Carmichael, J. Nicholls, A. L. Smith, Silica activity in igneous rocks. *Am. Mineral.* **55**, 246–263 (1970).
34. A. N. Krot, K. Nagashima, K. Fintor, E. Pál-Molnár, Evidence for oxygen-isotope exchange in refractory inclusions from Kaba (CV3.1) carbonaceous chondrite during fluid-rock interaction on the CV parent asteroid. *Acta Geogr. Geol. Meteorol. Debr. Geol. Gemorfol. Termeszfoldr. Sor.* **246**, 419–435 (2019).
35. G. S. Pokrovski, J. Roux, J.-C. Harrichoury, Fluid density control on vapor-liquid partitioning of metals in hydrothermal systems. *Geology* **33**, 657–660 (2005).
36. H. Palme, A. Jones, Solar system abundances of the elements. *Treatise on geochemistry.* **1**, 711 (2003).
37. P. A. Bland, M. D. Jackson, R. F. Coker, B. A. Cohen, J. B. W. Webber, M. R. Lee, C. M. Duffy, R. J. Chater, M. G. Ardakani, D. S. McPhail, D. W. McComb, G. K. Benedix, Why aqueous alteration in asteroids was isochemical: High porosity ≠ high permeability. *Earth Planet. Sci. Lett.* **287**, 559–568 (2009).
38. A. N. Krot, I. D. Hutcheon, A. J. Brearley, O. V Pravidtseva, M. I. Petaev, C. M. Hohenberg, *Timescales and Settings for Alteration of Chondritic Meteorites* (Lawrence Livermore National Lab.(LLNL), Livermore, CA (United States), 2005).
39. A. J. Ellis, Chemical equilibrium in magmatic gases. *Am. J. Sci.* **255**, 416–431 (1957).
40. J. Gmeling, Thermochemical data of pure substances, Part I/II. Von I. Barin. VCH, Weinheim – New York – Basel – Cambridge 1989. X, 1 829 S., 10 Abb., 2406 Tab., geb., DM 680. *Chemie Ing. Tech.* **62**, 644 (1990).
41. K. T. Howard, G. K. Benedix, P. A. Bland, G. Cressey, Modal mineralogy of CV3 chondrites by X-ray diffraction (PSD-XRD). *Geochim. Cosmochim. Acta* **74**, 5084–5097 (2010).
42. E. Tonui, M. Zolensky, T. Hiroi, T. Nakamura, M. E. Lipschutz, M.-S. Wang, K. Okudaira, Petrographic, chemical and spectroscopic evidence for thermal metamorphism in carbonaceous chondrites I: CI and CM chondrites. *Geochim. Cosmochim. Acta* **126**, 284–306 (2014).
43. A. N. Krot, E. R. D. Scott, M. E. Zolensky, Origin of fayalitic olivine rims and lath-shaped matrix olivine in the CV3 chondrite Allende and its dark inclusions. *Meteorit. Planet. Sci.* **32**, 31–49 (1997).
44. A. Garenne, P. Beck, G. Montes-Hernandez, L. Bonal, E. Quirico, O. Proux, J. L. Hazemann, The iron record of asteroidal processes in carbonaceous chondrites. *Meteorit. Planet. Sci.* **54**, 2652–2665 (2019).
45. L. Bonal, E. Quirico, M. Bourot-Denise, G. Montagnac, Determination of the petrologic type of CV3 chondrites by Raman spectroscopy of included organic matter. *Geochim. Cosmochim. Acta* **70**, 1849–1863 (2006).
46. G. J. MacPherson, K. Nagashima, A. N. Krot, P. M. Doyle, M. A. Ivanova, ⁵³Mn–⁵³Cr chronology of Ca–Fe silicates in CV3 chondrites. *Geochim. Cosmochim. Acta* **201**, 260–274 (2017).
47. N. T. Kita, T. Ushikubo, Evolution of protoplanetary disk inferred from ²⁶Al chronology of individual chondrules. *Meteorit. Planet. Sci.* **47**, 1108–1119 (2012).
48. J. Villeneuve, M. Chaussidon, G. Libourel, Homogeneous distribution of ²⁶Al in the solar system from the Mg isotopic composition of chondrules. *Science* **325**, 985–988 (2009).
49. K. Nagashima, A. N. Krot, M. Komatsu, ²⁶Al–²⁶Mg systematics in chondrules from Kaba and Yamato 980145 CV3 carbonaceous chondrites. *Geochim. Cosmochim. Acta* **201**, 303–319 (2017).
50. J. Pape, K. Mezger, A.-S. Bouvier, L. P. Baumgartner, Time and duration of chondrule formation: Constraints from ²⁶Al–²⁶Mg ages of individual chondrules. *Geochim. Cosmochim. Acta* **244**, 416–436 (2019).
51. B. Jacobsen, Q.-z. Yin, F. Moynier, Y. Amelin, A. N. Krot, K. Nagashima, I. D. Hutcheon, H. Palme, ²⁶Al–²⁶Mg and ²⁰⁷Pb–²⁰⁶Pb systematics of Allende CAIs: Canonical solar initial ²⁶Al/²⁷Al ratio reinstated. *Earth Planet. Sci. Lett.* **272**, 353–364 (2008).
52. K. A. Dyl, A. Bischoff, K. Ziegler, E. D. Young, K. Wimmer, P. A. Bland, Early Solar System hydrothermal activity in chondritic asteroids on 1–10-year timescales. *Proc. Natl. Acad. Sci. U.S.A.* **109**, 18306–18311 (2012).
53. L. T. Elkins-Tanton, B. P. Weiss, M. T. Zuber, Chondrites as samples of differentiated planetesimals. *Earth Planet. Sci. Lett.* **305**, 1–10 (2011).
54. L. Carporzen, B. P. Weiss, L. T. Elkins-Tanton, D. L. Shuster, D. Ebel, J. Gattacceca, Magnetic evidence for a partially differentiated carbonaceous chondrite parent body. *Proc. Natl. Acad. Sci. U.S.A.* **108**, 6386–6389 (2011).
55. J. Gattacceca, B. P. Weiss, M. Gounelle, New constraints on the magnetic history of the CV parent body and the solar nebula from the Kaba meteorite. *Earth Planet. Sci. Lett.* **455**, 166–175 (2016).
56. R. R. Fu, L. T. Elkins-Tanton, The fate of magmas in planetesimals and the retention of primitive chondritic crusts. *Earth Planet. Sci. Lett.* **390**, 128–137 (2014).
57. J. T. Armstrong, Quantitative analysis of silicates and oxide minerals: Comparison of Monte-Carlo, ZAF and Phi-Rho-Z procedures, in *Analysis Microbeam*, D. E. Newbury, Ed. (San Francisco Press, 1988), pp. 239–246.
58. C. De Capitani, K. Petrakakis, The computation of equilibrium assemblage diagrams with Theriak/Domino software. *Am. Mineral.* **95**, 1006–1016 (2010).
59. T. J. B. Holland, R. Powell, An improved and extended internally consistent thermodynamic dataset for phases of petrological interest, involving a new equation of state for solids. *J. Metam. Geol.* **29**, 333–383 (2011).
60. E. Jarosewich, Chemical analyses of meteorites: A compilation of stony and iron meteorite analyses. *Meteoritics* **25**, 323–337 (1990).

Acknowledgments: We thank A. Bernard for providing samples from Kudryavy fumarolic incrustations and the discussion on the Kudryavy volcano and fumarolic environments in general. The Museum National d'Histoire Naturelle (MNHN), Paris, the Statens Naturhistoriske Museum (Copenhagen), and the Smithsonian National Museum of Natural History (Washington, DC) are also thanked for the loan of CV chondrite thin sections. K. Nagashima is warmly acknowledged for the fruitful discussions and help in running the EMPA (HIGP, Honolulu, USA). We thank P. Michel for the careful reading of this manuscript. S. Jacomet (CEMEF, Mines ParisTech) and O. Tottereau (CRHEA, Nice, France) are also thanked for technical support. G.L. acknowledges funding support from the French space agency CNES as a science team co-investigator of the NASA OSIRIS-REx asteroid sample return mission. **Funding:** The BQR Géoazur (CG) and the Idex UCAJEDI Académie 3 from Université Côte d'Azur (CG) financially supported this study. **Author contributions:** G.L. discovered the similarity between the mineralogy of the Kudryavy fumarolic rocks and the Ca–Fe-rich secondary phases present in CV and CO chondrites that inspired this manuscript. C.G. and G.L. conceived and led this study, analyzed and interpreted the results, and wrote and corrected the manuscript. **Competing interests:** The authors declare that they have no competing interests. **Data and materials availability:** All data needed to evaluate the conclusions in the paper are present in the paper and/or the Supplementary Materials. Additional data related to this paper may be requested from the authors.

Submitted 31 January 2020

Accepted 20 May 2020

Published 3 July 2020

10.1126/sciadv.abb1166

Citation: C. Ganino, G. Libourel, Fumarolic-like activity on carbonaceous chondrite parent body. *Sci. Adv.* **6**, eabb1166 (2020).